

Climatic and tectonic controls on source-to-sink processes in the tropical, ultramafic catchment of Lake Towuti, Indonesia

Marina A. Morlock · Hendrik Vogel · Valentin Nigg · Luis Ordoñez ·
Ascelina K. M. Hasberg · Martin Melles · James M. Russell · Satria Bijaksana ·
the TDP Science Team

Received: 18 April 2018 / Accepted: 3 October 2018
© Springer Nature B.V. 2018

Abstract Humid tropical landscapes are subject to intense weathering and erosion, which strongly influence sediment mobilisation and deposition. In this setting, we aimed to understand how geomorphology and hydroclimate altered the style and intensity of erosion and sediment composition in a tropical lake and its tectonically active catchment. Lake Towuti (2.75°S, 121.5°E) is one of the oldest and deepest lakes in Indonesia, with uninterrupted lacustrine sedimentation over several glacial–interglacial cycles.

Electronic supplementary material The online version of this article (<https://doi.org/10.1007/s10933-018-0059-3>) contains supplementary material, which is available to authorized users.

M. A. Morlock (✉) · H. Vogel · V. Nigg
Institute of Geological Sciences and Oeschger Centre for
Climate Change Research, University of Bern, 3012 Bern,
Switzerland
e-mail: marina.morlock@geo.unibe.ch

H. Vogel
e-mail: hendrik.vogel@geo.unibe.ch

V. Nigg
e-mail: valentin.nigg@geo.unibe.ch

L. Ordoñez
Department of Earth Sciences, University of Geneva,
1205 Geneva, Switzerland
e-mail: Luis.Ordonez@unige.ch

Here we present results from a novel set of Lake Towuti surface sediment, bedrock and soil samples from the catchment, and two existing sediment cores that extend to 30,000 and 60,000 years before present. We studied the catchment morphology, soil properties, geochemistry, and clay and bulk mineralogy. Results from several river long profiles show clear signs of tectonic activity, which enhances river incision, favours mass movement processes, and together with remobilisation of fluvial deposits, strongly influences modern sedimentation in the lake. Material from the Mahalona River, the lake's largest inflow, dominates modern sediment composition in Towuti's northern basin. The river transports Al-poor

A. K. M. Hasberg · M. Melles
Institute of Mineralogy and Geology, University of
Cologne, 50674 Cologne, Germany
e-mail: hasberga@uni-koeln.de

M. Melles
e-mail: mmelles@uni-koeln.de

J. M. Russell
Department of Earth, Environmental, and Planetary
Sciences, Brown University, Providence, RI 02912, USA
e-mail: james_russell@brown.edu

S. Bijaksana
Faculty of Mining and Petroleum Engineering, Institut
Teknologi Bandung, Bandung 40132, Indonesia
e-mail: satria@fi.itb.ac.id

and Mg-rich sediments (mainly serpentines) to the lake, indicating river incision into the Mg-rich serpentinised peridotite bedrock. Relatively small, but important additional contributions of material, come from direct laterite-derived input and the Loeha River, which both provide Al-rich and Mg-poor sediment to the lake. Over time, the Al/Mg and kaolinite-to-serpentine ratios varied strongly, primarily in response to lake-level fluctuations driven by hydroclimatic changes. In the past 60,000 years, both the Al/Mg and kaolinite-to-serpentine ratios showed variations sensitive to changes in climate boundary conditions across glacial-interglacial cycles, while tectonic activity had less influence on changes in sediment composition on these short time-scales.

Keywords Laterite · Erosion · Hydroclimate · Lake Towuti · Lake level · Tropical palaeoclimate

Introduction

In the humid tropics, intense weathering results in a thick soil cover that is very susceptible to erosion by mass-wasting and high rainfall events. Soils provide an important resource for economic development in many (tropical) countries, both for agricultural use and mineral exploitation (U.S. Geological Survey 2017). Specifically, laterites are autochthonous weathering products characterised by high concentrations of immobile elements such as Fe and Al in the upper soil horizons (Widdowson 2007). There are several studies of laterite properties in tropical Africa (Ogunsanwo 1988; Omotoso et al. 2012; Adunoye 2014), but there is little known about how laterite properties influence erosion and sedimentary processes. Similarly, although a number of studies described the laterization of ultramafic bedrock (Golightly and Arancibia 1979; Colin et al. 1990; Brand et al. 1998; Sagapoa et al. 2011; Marsh et al. 2013), these studies often focused on ore exploration. The interaction between climate, soil properties, catchment geomorphology, and sedimentary processes has rarely been explored in laterite landscapes, and in the humid tropics in general.

Equatorial Lake Towuti (2.75°S, 121.5°E, 560 km², ~ 200 m maximum water depth; Fig. 1) is one of the oldest lakes in Indonesia (Von Rintelen

et al. 2012). The catchment geology consists of dunites, lherzolites, and harzburgites of the East Sulawesi Ophiolite complex (Kadariusman et al. 2004), upon which thick laterites have developed. Particles and solutes delivered to the lake are exceptionally rich in iron, but very poor in sulphur and macronutrients, setting the stage for unusual biogeochemical cycles, ultraoligotrophy, and a highly adapted, mostly endemic lake fauna and flora (Haffner et al. 2001; Crowe et al. 2008; Von Rintelen et al. 2012). Most of the lake is surrounded by dense, closed-canopy rainforest; however, based on satellite images, ~ 25% of the lake catchment is now deforested as a consequence of anthropogenic activities. Previous studies of Lake Towuti suggest that during the past 60,000 years, hydrologic changes driven by changing global climate boundary conditions had large impacts on lake sedimentation (Russell et al. 2014; Vogel et al. 2015). Lake-level lowstands were accompanied by delta progradation into the deeper basins, which favours lateral transport processes relative to pelagic sedimentation (Vogel et al. 2015). This change in depositional modes leads to coarser-grained sediments in the deeper basins and associated changes in mineralogy (Weber et al. 2015; Goudge et al. 2017). In 2015 the International Continental Scientific Drilling Program (ICDP) Towuti Drilling Project (TDP) recovered cores through the entire sediment infill of Lake Towuti, which record uninterrupted lacustrine sedimentation over several glacial-interglacial cycles (Russell et al. 2016).

We carried out novel analyses of bedrock and soil samples from Lake Towuti's catchment, along with geomorphological analyses, to characterise and understand modern source-to-sink processes around this tropical lake system. We analysed the inorganic geochemistry, clay and bulk mineralogy, and sedimentological characteristics of bedrock, soils, and lake surface sediment and core samples to disentangle the effects of climatic and tectonic processes and their influence on erosion and sedimentation. We applied this understanding to interpret mineralogical and geochemical variations in two sediment cores that extend 30 and 60 kilo years before present (kyr BP). This study links modern sedimentation processes to existing and new palaeoclimate reconstructions from Lake Towuti to better understand modern tropical lake systems and how such systems change under different climate boundary conditions. Such a study is timely,

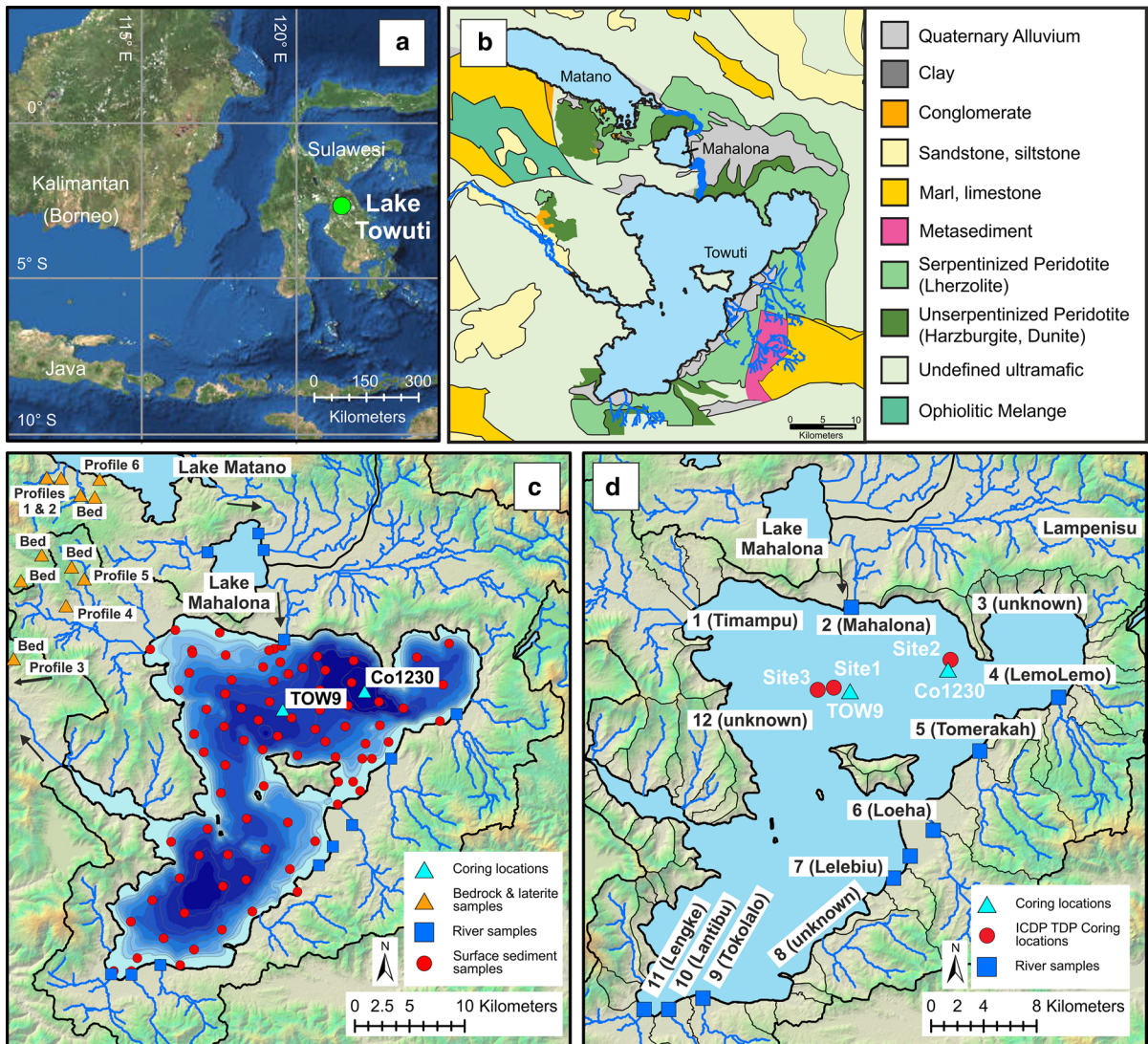


Fig. 1 (a) Location of Lake Towuti on the island of Sulawesi, Indonesia. (b) Geologic map of the Malili lake system with Lake Towuti and upstream Lakes Mahalona and Matano, modified after Costa et al. (2015). (c) Map of the sampling locations

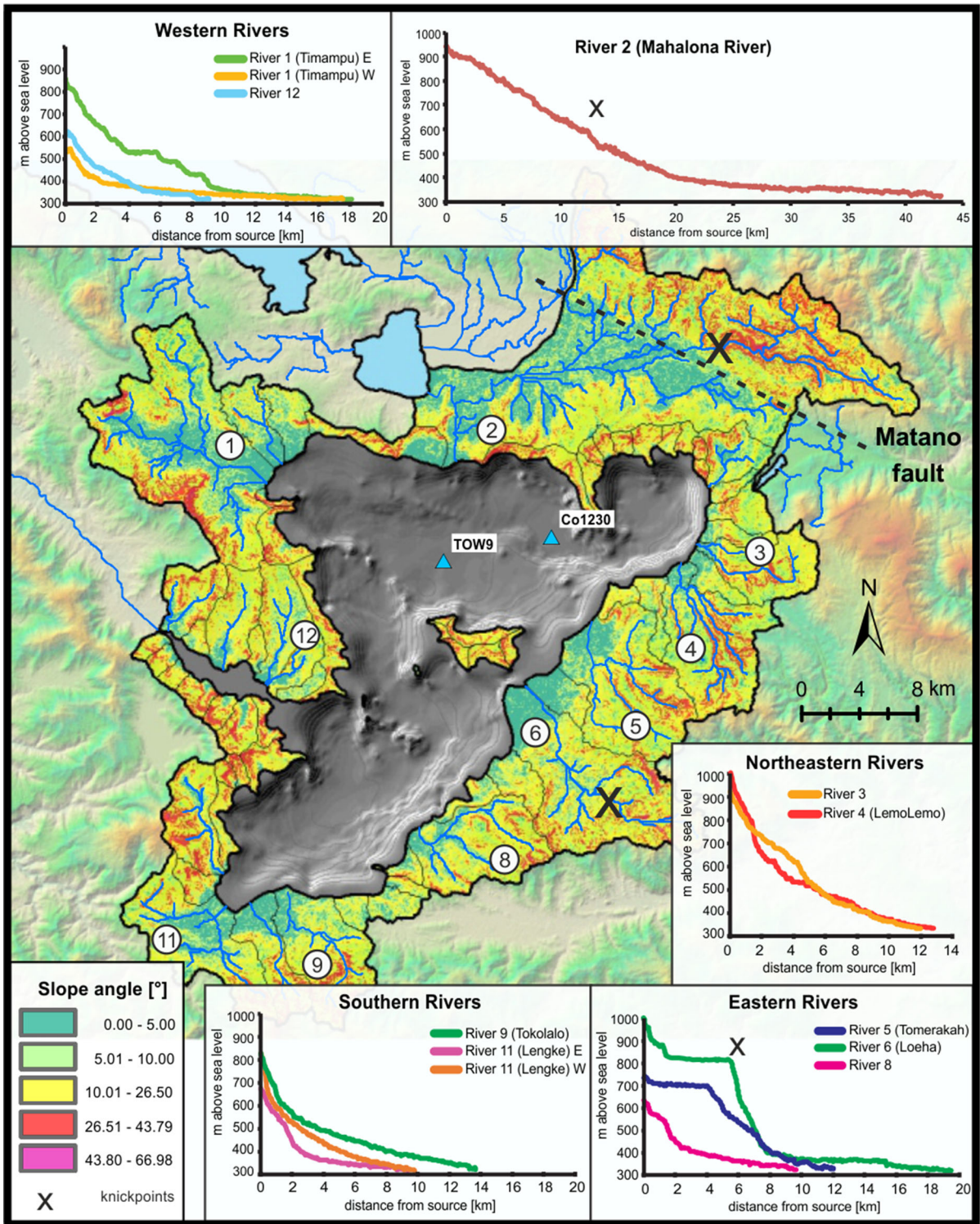
around Lake Towuti; data for river bedload (squares) from Costa et al. (2015). (d) Map of Lake Towuti, with river names and sampling locations. Red circles indicate the three coring sites of the ICDP Towuti Drilling Project

given the unprecedented rates of anthropogenically induced change that tropical regions are currently undergoing.

Hydrologic setting

Lake Towuti is part of the Malili Lake System, a chain of five tectonic lakes located on the island of Sulawesi, Indonesia (Fig. 1). The lake receives annual precipitation of ~ 2700 mm, with peak rainfall (~ 330 mm/month) in austral autumn (MAM), and

comparatively dry (~ 140 mm/month) austral spring months (ASO; Konecky et al. 2016). Lake Towuti is a hydrologically open lake with one outflow, the Larona River (Fig. 1c). The lake is split into two connected major basins to the north and south (Figs. 1c and 2), which are separated by bedrock highs above and below the current water surface (Vogel et al. 2015; Russell et al. 2016). To the north, the lake is connected to upstream Lakes Matano and Mahalona via the Mahalona River (Fig. 1d), which dominates water and sediment input to Towuti’s northern basin (Costa et al.



◀ **Fig. 2** Slope angles [°] in the Lake Towuti catchment. Colour classification is partly based on the critical angle of internal friction as determined in direct shearing tests on the sampled laterite material (26.5° and 43.79° for upper and lower laterite horizons, respectively). Slope data are based on the DEM. Insets: Long profiles of all major rivers flowing into Lake Towuti. Profiles are based on DEM analysis and were computed by the ArcGIS 10.1 hydrology toolset. (Color figure online)

2015). The large catchment of the Mahalona River includes the Lampenisu River catchment, which is characterised by Quaternary alluvium and partly serpentinitised peridotites. Together, the two rivers comprise 25% (293 km²) of the catchment area of Lake Towuti, excluding the catchments of Lakes Matano and Mahalona. Despite severe drying during the last glacial maximum (Russell et al. 2014) and associated lake-level lowstands, the lake remained hydrologically connected to upstream lakes via the Mahalona River throughout the last 60,000 years (Costa et al. 2015). Lake Towuti's southern basin has four prominent inflows. The Loeha River drains a catchment hosting metasedimentary rock to the east of the lake, the only source of felsic minerals in the catchment of Lake Towuti (Fig. 1b and d, Costa et al. 2015). Three rivers at the southern tip of the lake jointly drain 10% of the lake's catchment and are underlain by ultramafic rocks. Lake Towuti's western and northeastern shores are dominated by steep slopes and densely vegetated catchments with no major permanent river drainage (Fig. 1d).

Materials and methods

Geotechnical and geomorphological analysis

River and catchment morphology were analysed using a digital elevation model (DEM) of the Lake Towuti region. The DEM is based on data from NASA's Shuttle Radar Topography Mission at 1 arc-second (30 m) spatial resolution (available at: <http://earthexplorer.usgs.gov>, last accessed: February 09 2017). Rivers and catchment boundaries were identified using the hydrology toolset in ArcGIS 10.1 (Esri, USA). Catchment sizes, river lengths, trunk channel relief, and long profiles were calculated based on this DEM data set.

In total, 18 bedrock samples (from 12 locations) and 6 laterite profiles (21 samples) were collected in May–July 2015 (Fig. 1c). Samples cover varying degrees of serpentinitisation of the peridotite bedrock and represent all the vertical zones of the laterites. Because of accessibility, all samples were taken northwest of the lake (Fig. 1c). Representative laterite samples, formed on serpentinitised and non-serpentinitised peridotites, were dried at 110 °C overnight and their plasticity index (I_p), grain-size distributions, soil cohesion (c), and friction angle (angle of internal friction ϕ) were determined at the geotechnical laboratory of the Bern University of Applied Sciences in Burgdorf, Switzerland. Grain-size data were acquired following Swiss norms SN 670 816a and SN 670 902-1. Samples were treated with 15 ml Na(PO₃)₆ for 24 h before settling, wet, and dry sieving. The resulting grain-size distribution curves were categorized following the Unified Soil Classification System and corresponding geotechnical parameters were selected according to Swiss Norm SN 670 010. The parameters ϕ and c were determined in repeated direct shearing tests, for which varying loads (20, 40, and 80 kN) were applied to the samples for 20 h before samples were sheared at a rate of 1 mm per minute under undrained conditions (German Industrial Norm DIN 18137-1 and DIN 18137-3). To calculate the plasticity index, plastic and liquid limits of samples were determined following Swiss Norm SN 670 345b, which follows Casagrande (1932).

Surface sediment collection and sediment coring

In 2015, 84 surface sediment samples from across the entire lake were recovered from water depths between 2.8 and 195.5 m with a grab sampler. Samples integrate the uppermost 3–5 cm of recovered sediment, representing 200–250 yr of sediment accumulation in the deep basins (Russell et al. 2014; Vogel et al. 2015). Core Co1230 (19.8 m long, base ¹⁴C-dated to 27 kyr BP) was recovered from a distal position to the Mahalona River Delta in the northern basin at ~ 203 m water depth in 2010 (Vogel et al. 2015). Core IDLE-TOW10-9B-1 K (hereafter TOW9) was recovered from 154 m water depth. This 11.5-m core was dated to ~ 45 kyr BP by ¹⁴C dating at 8.95 m depth, and the sedimentation rate over this interval was extrapolated to an age of 60 kyr BP for the core base (Russell et al. 2014).

Geochemistry and grain size

The geochemical composition of bedrock, laterite, lake surface sediment samples, and sediment samples from core Co1230 was determined by inductively coupled plasma mass spectrometry (ICP-MS) after full acid digestion (HF, HCl, HNO₃, HClO₄) of the samples at the Activation Laboratories Ltd. in Ontario, Canada. Because detection limits were reached for many elements in bedrock and laterite samples, these samples were also measured with wavelength dispersive X-ray fluorescence (WD-XRF), and results are reported for concentrations of K, Mg, Cr, and Ni. For WD-XRF analysis, samples were ground in an oscillating tungsten-carbide mill, dried in an oven at 100 °C for 12 h, and heated to 1050 °C for two hours. Of the burnt rock powder 1.2121 g were mixed with 6.0000 g of lithium-tetraborate (Li₂B₄O₇), placed in a Pt–Au crucible and melted in a Bead Machine (Perl X'3) at 1250 °C. Major element concentrations were analysed on a Philips PW2400 WD-XRF spectrometer at the University of Lausanne, Switzerland. The lower detection limit is 0.01 weight-% (wt%) for all elements. The geochemical composition of the bedload of eight rivers is available from Costa et al. (2015), and Goudge et al. (2017) provide grain-size specific chemical and mineralogical data on bedload and suspended load for the Mahalona River. Geochemistry of sediment core TOW9 is available from Russell et al. (2014).

Based on the ICP-MS measurements, we calculated the Chemical Index of Alteration (CIA) of Nesbitt and Young (1982) as a measure of the degree of chemical weathering of different samples. The index is based on the relative accumulation of the less mobile Al₂O₃ relative to more easily soluble Na₂O, K₂O, and CaO_{silicate} in a weathered substrate, e.g. bedrock, soil or sediment. Because calcareous rocks are largely absent in the catchment of Lake Towuti and petrographic observations do not indicate the presence of detrital CaCO₃, we assumed all CaO in the system is derived from silicate rocks (CaO_{silicate}). Grain-size measurements of sediment core Co1230 are available from Vogel et al. (2015), who analysed the samples on a laser diffractometer (Malvern Mastersizer 2000S). The grain-size distribution of lake surface sediments was measured at the University of Cologne, Germany, with a Beckman Coulter LS13320 laser

diffractometer. Samples were treated with 15 ml H₂O₂ (30%), 10 ml HCl (10%) and NaOH (1 M) prior to analysis.

Bulk and clay mineralogy

One representative laterite profile over both serpentinised and unserpentinised peridotite bedrock, respectively, was analysed for bulk mineralogy by x-ray diffraction (XRD) on a PANalytical Cubix³ goniometer with a Cu-tube and a monochromator (45 kV, 40 mA, 5°–60° 2θ). The bulk mineralogy of a lake surface sediment transect from the Mahalona River mouth to coring site TOW9 was determined by XRD on a PANalytical X'Pert Pro with a Cu X-ray tube (40 kV, 40 mA, 5°–60° 2θ). Prior to analysis, freeze-dried samples were mixed and homogenized with 10 wt% LiF to provide a standard for peak integration and quantification. Additionally, thin sections of bedrock and saprolite zone samples were examined with a polarizing light microscope.

Clay mineralogical analyses were performed on all sediment samples. The < 2-μm size fraction (clay size) was separated from the sample by Atterberg separation (Robinson 1922; ~ 0.5 g of sample, 4.5-h settling time, 6-cm settling height, 21 °C). For XRD analyses on oriented clay mounts, the clay fraction was added to three glass plates and dried overnight. One glass plate was measured immediately on a Phillips PW1830 Goniometer (40 kV, 30 mA, 2°–40° 2θ), another plate was kept in an ethylene-glycol-saturated atmosphere for at least 48 h prior to measurement, and one plate was heated at 550 °C for 1.5 h before measurement (Electronic Supplementary Material [ESM] Fig. S1a). By comparing the three treatment spectra, we identified characteristic peaks for smectites (5.2° 2θ), illite (8.8° 2θ), serpentines (12.24° 2θ), and kaolinite (12.5° 2θ) in the ethylene-glycol-saturated spectrum (ESM Fig. S1a). Kaolinite and serpentine peaks were separated using peak separation software (MacDiff, R. Petschick, Frankfurt, Germany, 2001), the output being peak height in absolute counts. Only selected XRD measurements were done for the highly cemented laterite samples. To further evaluate the interpretation and separation of kaolinite from serpentine minerals by XRD analysis, clay separates of core Co1230 and all bulk samples were also measured by mid-infrared (MIR) Fourier-Transform-Infrared-Spectroscopy (FTIRS). For this,

0.011 ± 0.0001 g of freeze-dried material was mixed with 0.5 ± 0.0005 g of spectroscopic grade KBr and homogenised for at least three minutes. FTIRS analyses were performed at the University of Bern, Switzerland, using a Bruker Vertex 70 equipped with an HTS-XT accessory unit, a liquid nitrogen cooled MCT (Mercury-Cadmium-Telluride) detector, and a KBr beam splitter, in the wavenumber range 3750–520 cm⁻¹ at a resolution of 4 cm⁻¹. All measurements were performed in diffuse reflectance mode. Several mineral-characteristic absorbance peaks appear as prominent features in the Towuti samples. Diagnostic peaks for kaolinite were centred at 692, 913, 3620 cm⁻¹, caused by translational, librational, and stretching vibrations of OH groups, respectively, in kaolinite group minerals (Chester and Elderfield 1973; Farmer 1974; Madejová 2003; Chukanov 2014). Identified absorbance peaks diagnostic for serpentine group minerals were centred at 640, 958, and 3685 cm⁻¹, caused by bending, libration, and stretching vibrations of OH, respectively (Farmer 1974; Madejová 2003; Chukanov 2014). Peak integrals of diagnostic peaks are highly correlated for the individual mineral groups, emphasizing that absorbance in the analysed regions is diagnostic for the respective mineral group, without significant bias from other phases absorbing in the same region (Chester and Elderfield 1973). For further analysis, peak areas with highest correlation to clay XRD and geochemical composition were chosen. These were peaks at wavenumbers 900.8–924.6 cm⁻¹ for kaolinite and 3674.9–3694.2 cm⁻¹ for serpentine.

Statistics and data analysis

All statistical analyses were performed in R (R Development Core Team 2008). For Pearson correlation tests, normality of the variables was tested with the Shapiro–Wilks test. If the data were not normally distributed, Spearman's rank correlation was used to test for correlations. Statistical parameters are given as mean and one standard deviation. All maps were created in ArcGIS 10.1 (Esri, USA). Unless otherwise stated, interpolation of the surface sediment measurements is based on Kriging (Gaussian process regression) with a fixed radius of 5 km and a minimum of 5 data points used for calculations. Raster size is 50 × 50 m. A geometrical classification was chosen for data visualisation.

Results

Catchment morphology

The three connected lakes of the Malili Lake System (excluding its two satellite lakes) drain a hydrologic catchment area of 2430 km². Upstream lakes and their surroundings account for a catchment area of 1286 km². We assume that Lakes Matano and Mahalona function as sediment traps, providing water, but little sediment, leaving an area of 1144 km² to supply the majority of sediment to Lake Towuti (ESM Table S1). Rivers drain 86% of Towuti's catchment (excluding upstream lake catchments), whereas 14% of the area may be drained by surface runoff and/or ephemeral streams, or is left undrained. The catchments around Lake Towuti have mean slope angles between 13.1° and 16.8° (Fig. 2, ESM Table S1). The trunk channel relief (as defined by Whipple et al. 1999) varies between 150 and 680 m over distances from 5 to 43 km. Excluding the catchments that feed into upstream Lakes Matano and Mahalona, the Mahalona River drains the largest catchment (293 km² catchment size, 43 km length, 14.5° average catchment slope), the majority of which consists of the Lampenisu River, followed by the Timampu River (141 km² catchment size, 18 km length, 13.1° average catchment slope) and the Loeha River (84 km² catchment size, 21 km length, 15.5° average catchment slope). Several knickpoints are present in the river courses to the east of Lake Towuti (Fig. 2). Most prominent, the Loeha River drops by 400 m over a distance of 2.5 km (average river slope 9.1°). Along the Lampenisu River profile, the Matano Fault, a highly segmented, sinistral strike-slip fault with an extensional component (Watkinson and Hall 2016), creates an elevation offset of about 50 m over a distance of 400 m (average river slope 7.1°), which is also clearly visible in an abrupt change of slope angle in the northern part of the Lampenisu River catchment (Fig. 2). Rivers to the south and northwest have well-developed river profiles. The three major rivers, the Mahalona (north), Loeha (east), Timampu (northwest), and the southernmost rivers, have wide alluvial plains in their lower course. Observations during fieldwork in 2015 indicated that the rivers on these alluvial plains presently cut into fluvial gravel deposits and have wide stream channels with exposed gravel bars along both sides of the active channel.

Laterites

The six laterite profiles investigated (Fig. 3, ESM Fig. S2) varied in thickness between 2 and 6 m and show a clear colour zonation with the uppermost horizon characterised by dark red material (approximately 0.2–1 m thick, 6 samples). Going deeper, this grades into a lighter red colour (0–1 m thick, 5 samples), followed by a yellow intermediate zone (1–2 m thick, 7 samples), then a green-grey-coloured saprolite zone (0.5–3 m thick, 5 samples) just above the unweathered parent rock. The colour zonation is very clearly reflected in elemental gradients, which are similar in soil profiles over varying degrees of bedrock serpentinisation (Fig. 3, ESM Fig. S2). In the laterites, Al, Fe, Ti, K, Cr, Zr, Zn, and Mn are enriched relative to the saprolite and bedrock, peaking in the red rather than the uppermost dark red zone (Fig. 3 and ESM Fig. S2). In contrast, Mg and Ca have the highest concentrations in the saprolite and bedrock, and decrease markedly upwards in the laterite (Fig. 3 and ESM Fig. S2). Nickel concentrations peak in the saprolite zone with an average concentration of $1.5 \pm 1.1\%$. Laterite profiles 1, 3, and 4 are located on slopes and coarse pebbles were visible in the dark red matrix of the uppermost zone, but the pebbles were

not included in the samples used for analysis. Average concentrations of Al ranged from $4.3 \pm 1.2\%$ in the uppermost dark red horizon to $0.9 \pm 0.9\%$ in the bedrock. Likewise, Fe (dark red zone: $32.8 \pm 15.8\%$; bedrock: $5.8 \pm 0.3\%$) and Ti (dark red zone: $0.1 \pm 0.06\%$; bedrock: $0.03 \pm 0.05\%$) were concentrated in the laterite relative to unweathered bedrock. Mg concentrations increased from $6.8 \pm 6.5\%$ in the uppermost horizon to $39.3 \pm 6.3\%$ in the bedrock. The CIA shows strongly increasing values from bedrock (mean 33.6 ± 15.3) to the overlying laterite (mean 94.0 ± 9.1).

Bulk XRD and thin section analyses show that unserpentinised rocks consist of olivine (> 60%), clino- and orthopyroxenes (diopside and enstatite, 10–25%), and small amounts (< 5%) of accessory minerals such as magnetite, illmenite, amphiboles, and goethite. Parts of the bedrock have undergone secondary serpentinisation close to the surface (ESM Fig. S3a). The main mineral phases in serpentinised samples are chrysotile and antigorite, with small amounts of magnetite and chlorite. In places, initially serpentinised peridotites have undergone a second alteration to form very fine-grained olivine and amphiboles (tremolite). In the weathering crust of the bedrock samples, serpentine and magnetite rinds

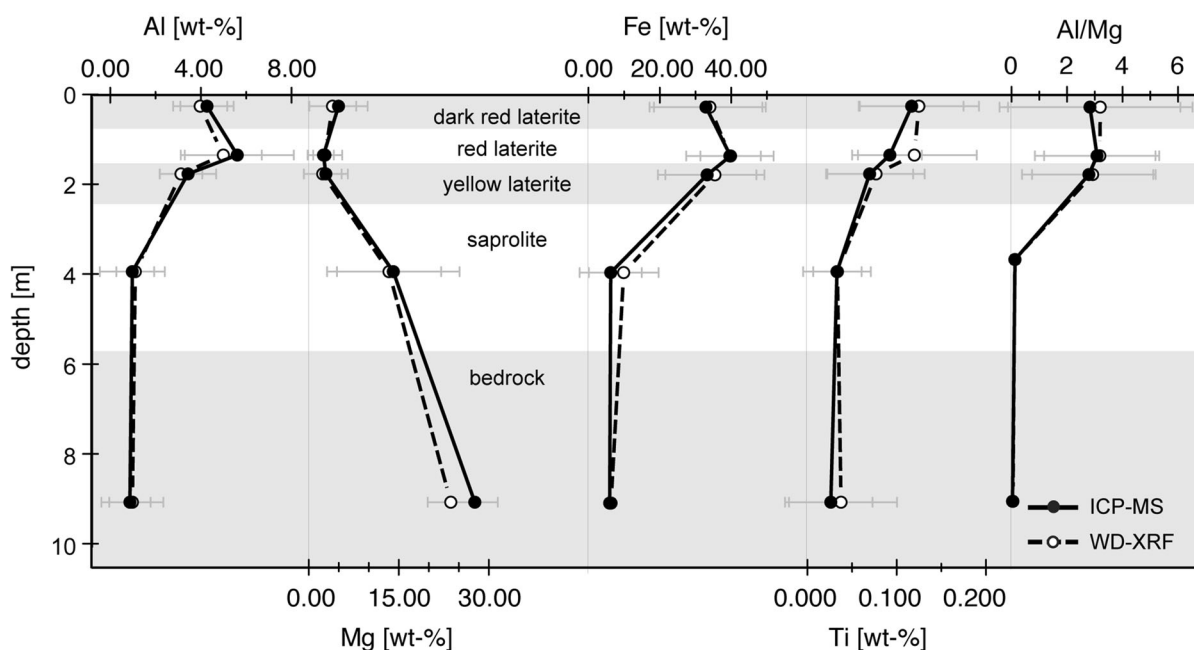


Fig. 3 Average element concentrations of six laterite profiles (for data from individual profiles, see Fig. S5). Depth is the average depth of each of the five zones. Error bars correspond to \pm one standard deviation

are observed around disintegrating olivine grains (ESM Fig. S3c). Small amounts of (clino)pyroxenes and amphiboles remain present in the saprolite and lower laterite zone. Veins in the saprolite and laterite are filled with very fine-grained secondary quartz crystals (ESM Fig. S3b). In the laterite horizons, goethite is the dominant mineral phase (ESM Fig. S4), and smectites are present in the yellow laterite horizon (ESM Fig. S4). FTIR spectroscopy further indicates the presence of kaolinite in the upper laterite horizons, whereas serpentines are more common in the lower laterite and saprolite zone (ESM Fig. S2c).

Geotechnical parameters of the laterites are summarised in ESM Fig. S5. Grain-size distribution curves are classified as *silt with sand* (ML) for sample Lat 8 a + b (profile 4, red and yellow laterite zone), *elastic silt* (MH) for sample Lat 9 b + c (profile 5, red and yellow laterite zone), *silty sand* (SM) for sample Lat 10 b + c and Sap 3 (profile 6, red laterite zone, and profile 2, saprolite zone, respectively), and *elastic silt with sand* (MH) for sample Lat 10 d + e (profile 6, yellow laterite zone). Coarse fractions (> 0.063 mm) of all five samples are dominated by magnetite grains, with occasional quartz and metal oxide concretions. The internal angles of friction (ϕ) for samples Lat 10 b + c (red laterite horizon) and 10 d + c (yellow laterite horizon) are 43.8° and 26.5° , respectively, with material density of 2.3 and 1.5 g cm $^{-3}$, respectively. The ϕ -angles based on classification of grain size distribution curves are 34° in the saprolite zone, 25° – 28° in the lower (lower red and yellow zone combined), and 33.6° in the upper laterite (dark red and upper red zone combined) horizons. Plasticity indices (I_p) are around 5% in the upper laterite horizon and saprolite zone, and 20–35% in the lower laterite horizon. Water content is 9.8% in the saprolite zone, between 44.3 and 104.2% in the yellow laterite horizons, and 17.9% in the red laterite horizon.

Lake surface sediments

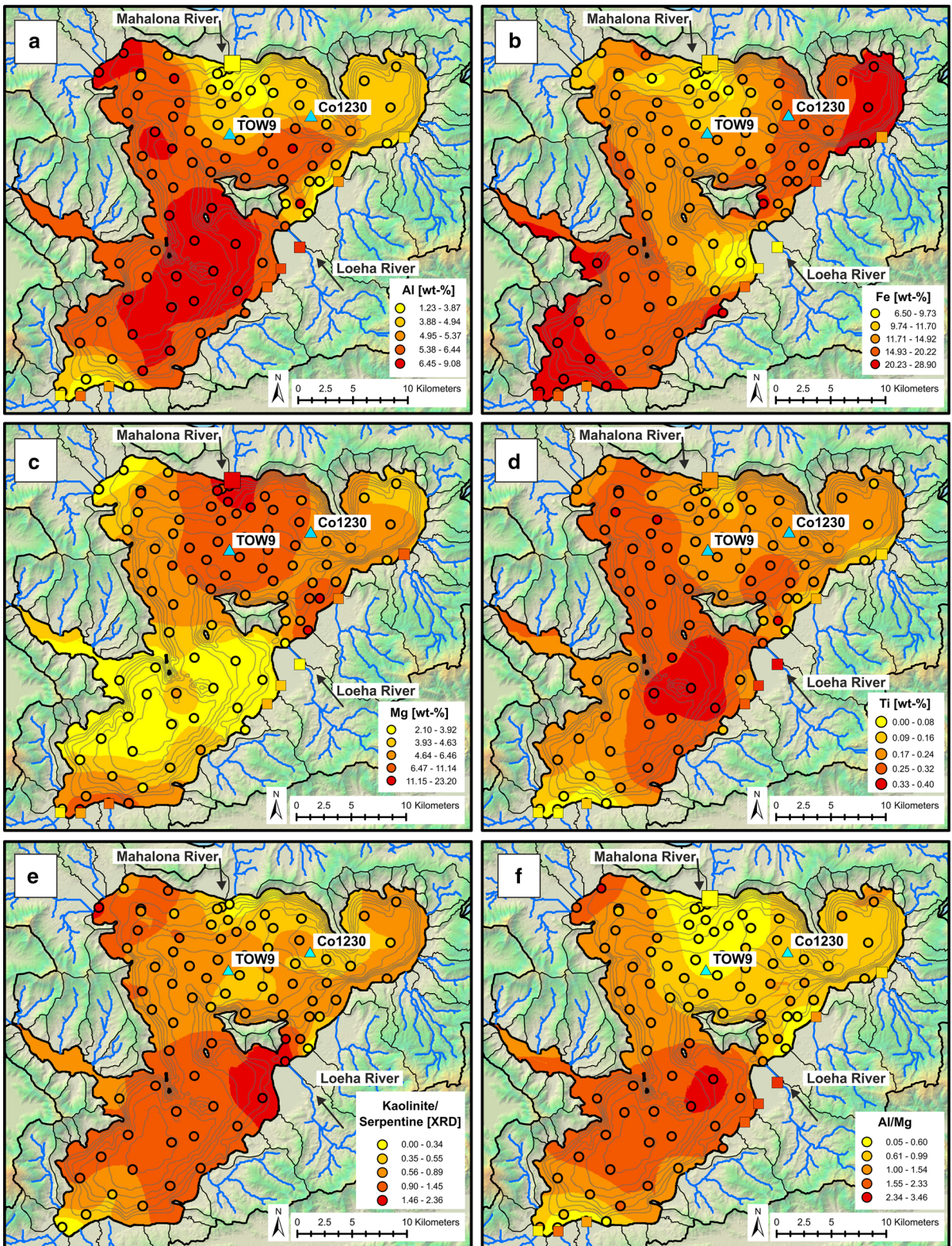
Lake surface sediments close to the Mahalona River inflow are characterised by high Mg concentrations, whereas Al, Ni, and Fe concentrations are low (Fig. 4 and ESM Fig. S6). This pattern decreases with increasing distance from the river mouth. Similarly, sediments at the southern tip of the lake are depleted in Al and Ti, and enriched in Mg (Fig. 4). In general, coarser-grained samples show a closer resemblance to

bedrock samples, whereas the elemental composition of fine-grained samples is more similar to the composition of the laterites (Fig. 4, ESM Fig. S6). The lake surface sediments have a mean CIA of 79.3 ± 8.6 . Values are lowest close to the inlets of the Mahalona and Loeha Rivers (CIA < 70), and peak in the northeast and south of the lake (CIA > 85 ; ESM Fig. S6b). Delta sediments of the Loeha River are characterised by low concentrations of Ni, Cr, Co, and Fe and high concentrations of K, Ti, Al, Sb, and Sr (Fig. 4, ESM Fig. S6, and Hasberg et al. 2018). Except for isolated patches close to shore, e.g. close to the Mahalona River inflow, Al, Ni, and Ti concentrations are mostly homogenous across the lake (Fig. 4 and ESM Fig. S6). Ca and Mg concentrations are generally higher in the northern (Ca: 0.72%; Mg: 7.13%) compared to the southern (Ca: 0.45%; Mg: 5.33%) lake basin.

The kaolinite-to-serpentine ratio is high in sediments off the Loeha River inflow and in areas without significant riverine runoff, whereas values are lower close to the Mahalona River and at the inflow of the southernmost rivers (Fig. 4e and ESM Fig. S6g). Clay mineralogical analysis shows general agreement between XRD results of the clay fraction (peak height) and bulk MIR-FTIRS measurements (peak area) for kaolinite and serpentine (Pearson correlation $r = 0.50$, and Spearman's rank correlation $r = 0.69$, respectively, $p < 0.01$, $n = 79$, ESM Fig. S1), and also between clay XRD results and Al and Mg concentrations in the bulk sediment (Pearson correlation $r = 0.56$, and Spearman's rank correlation $r = 0.64$, respectively, $p < 0.01$, $n = 79$, ESM Fig. S1). Bulk XRD analyses show a decrease in serpentines and amphiboles and an increase in quartz content (ESM Fig. S7) with distance from the Mahalona River, indicating that key elements are related to main mineral composition. The smectite-to-illite ratio is generally lower in the southern lake basin, especially around the Loeha River, whereas smectite is enriched relative to illite in the northern basin (ESM Fig. S6h).

Sediment cores

Coring location Co1230 is more heavily influenced by hypopycnal flows and turbidite deposition from the Mahalona Delta compared to coring location TOW9 (Vogel et al. 2015). The fine-grained pelagic sediments of the two cores, however, show very similar



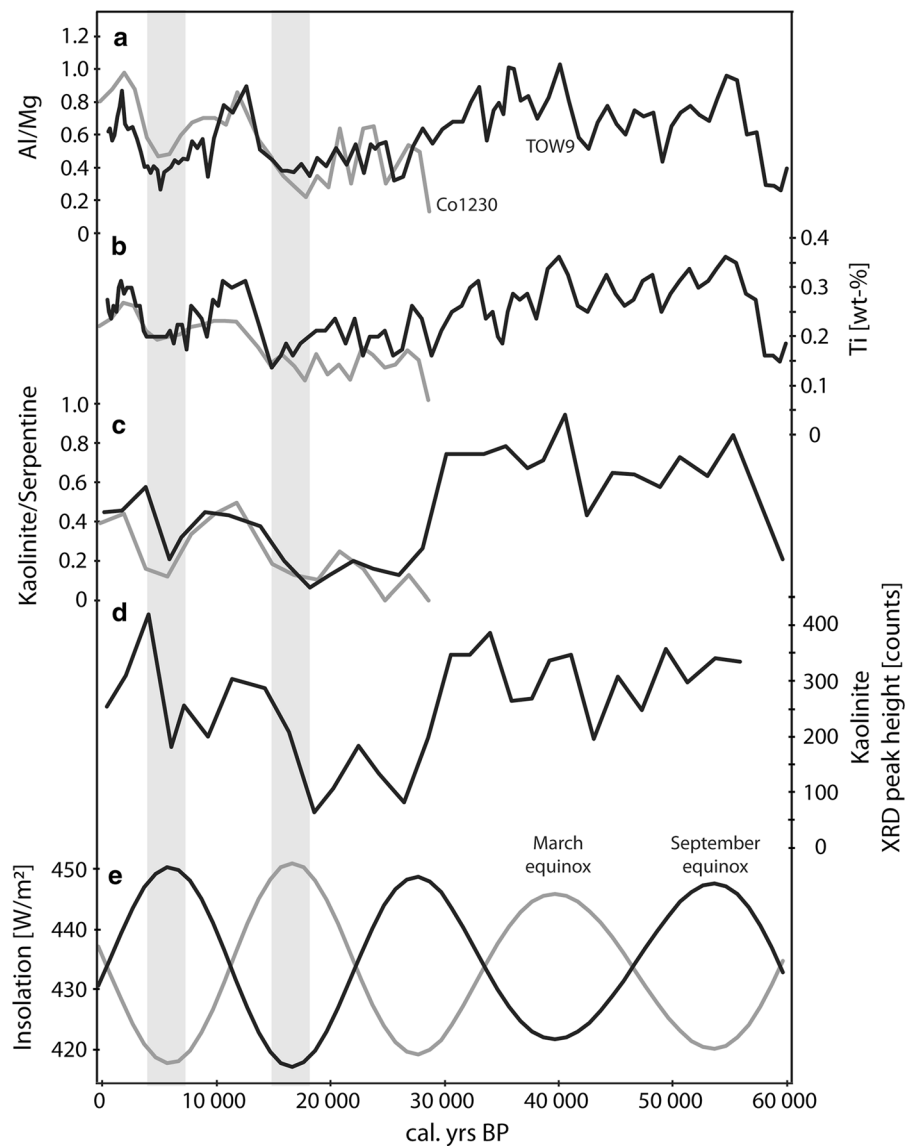
◀ **Fig. 4** (a)–(d) Element concentrations of Al, Fe, Mg, and Ti determined by ICP-MS, (e) kaolinite-to-serpentine ratio determined by clay XRD and f Al/Mg ratio determined by ICP-MS on 84 surface sediment samples, indicated by colour-coded circles. Background colouring is based on kriging interpolation of the surface sediment measurements. Grey lines represent the lake bathymetry with a 20-m line spacing (maximum water depth is ~ 200 m), data for river bedload (squares) from Costa et al. (2015), symbol size is scaled to catchment size (no data available for clay minerals). (Color figure online)

trends in their geochemical composition. The Al/Mg ratio is low in the middle to late Holocene (6–4 kyr BP), between 27 and 15 kyr BP, and prior to 58 kyr BP

(TOW9 only, Fig. 5a). High Al/Mg values occur at 2 and 13–11 kyr BP, between 41 and 32 kyr BP, and at 55 kyr BP. Ti concentrations show a similar pattern, which is overlain by an overall decreasing trend from 55 to 15 kyr BP (Fig. 5b, Russell et al. 2014).

Kaolinite and serpentine measured by clay-size MIR-FTIRS (band depth) and clay XRD (peak height) in Co1230 are strongly correlated (Pearson correlation $r = 0.77$, and $r = 0.73$, respectively, $p < 0.01$, $n = 14$, ESM Fig. S1), as are clay XRD kaolinite and serpentine with concentrations of bulk Al and Mg (Pearson correlation $r = 0.71$, and $r = 0.87$, respectively, $p < 0.01$, $n = 15$, ESM Fig. S1). Core TOW9

Fig. 5 (a) Al/Mg ratio, (b) Ti concentrations, (c) kaolinite-to-serpentine ratio, and (d) kaolinite content determined by clay XRD, of the two sediment cores, Co1230 and TOW9. The cores are located close to the two main sites of the ICDP Towuti Drilling Project (Fig. 1d). (e) Mean daily insolation for March and September equinoxes at 2°S



shows coherent trends in clay XRD kaolinite and serpentine and concentrations of Al and Mg over the past 60 kyr (Fig. 5a and c), but clay XRD and geochemical concentrations were not determined on the same sediment horizons, precluding analysis of correlation. The kaolinite-to-serpentine ratio is generally higher between 55 and 27 kyr BP compared to 27–0 kyr BP and prior to 58 kyr BP. For the past ~ 40 kyr, a similar pattern appears for kaolinite and serpentine, determined by near-infrared spectroscopy on other sediment cores from Towuti's northern basin (Goudge et al. 2017).

Discussion

Weathering and erosion processes in Lake Towuti's catchment

The laterite profiles around Lake Towuti closely follow a geochemical and mineralogical zonation characteristic of well-developed tropical laterites (Colin et al. 1990; Brand et al. 1998; Marsh et al. 2013). We did not observe major differences in laterite zonation and elemental composition between the laterites across varying degrees of bedrock serpentinisation (ESM Fig. S2). Bedrock and laterite mineralogy indicate that olivine weathers readily whereas pyroxene remains present in the saprolite zone and lower laterite horizons. Veins in the saprolite and laterite consist mainly of secondary quartz (ESM Fig. S3) and may thus serve as a quartz source to the lake sediments in the ultramafic part of the lake catchment. Very high goethite concentrations in the upper laterite horizon and steep element concentration gradients through the laterite horizons indicate that most other components have been transformed or leached from the profiles (Golightly and Arancibia 1979; ESM Fig. S4).

Peak elemental concentrations in the red rather than the uppermost dark red zone of laterite profiles from slope positions, e.g. in Fe and Al (Fig. 3, ESM Fig. S2a), suggest surficial reworking by slope processes. Coarse pebbles in the uppermost zone of some profiles support the idea of potential input of less weathered material from upslope positions. Features of slope processes, including slope creep and mass wasting, were clearly visible during fieldwork. Slopes with a steepness above the

empirically determined critical angle of friction (25° – 43° , i.e. areas that exceed the Mohr–Coulomb failure criterion) are found throughout the catchments and suggest that slope processes such as landslides are a prevalent feature in catchments around Lake Towuti and possibly similarly structured tropical catchments. Geotechnical analyses of the laterites around Towuti (ESM Fig. S5) suggest that upper laterite horizons have a larger grain size, lower water uptake capacity (I_P of ~ 5%), and are stable at higher slope angles (ϕ -angle 43.8°) compared to clay-rich lower laterite horizons with water content of up to 100% (I_P of 18–20%) and a low (26.5°) critical angle of internal friction. Our analysis suggests that lower laterite horizons fail more readily compared to upper soil layers and thus function as a slip plane, mobilising the entire soil package when slope failures occur.

Seismicity-induced slope failure has been recognised as an important process in the erosion of tropical landscapes (Thomas 1996), and in Lake Towuti's active tectonic setting, strong earthquakes occur regularly (Jones et al. 2014). Recently, a shallow-focus M_W 6.1 earthquake occurred in 2011 at the shore of Lake Matano, with a potential surface rupture length of 39 km (Watkinson and Hall 2016). Detailed tectonic studies of the area are still lacking, but geomorphologic evidence and fault kinematics analyses suggest rapid slip rates along the Matano fault and activity throughout the Quaternary (Bellier et al. 2006). Our analysis therefore suggests seismically triggered slope failures are important to erosion and sediment supply in tectonically active landscapes. In such environments, fault activity and seismic events enhance the mobilisation of the entire soil package, despite dense vegetation cover, and facilitate erosion of fine-grained soil material below the compacted upper laterite crust. In addition, slope processes also contribute directly to sedimentation in near-shore areas. Especially in the W and NE of the lake, steep slopes are located close to the lakeshore, such that mass movement material can directly reach the lake without intermediate fluvial transport and sorting of the material. During fieldwork in 2015, several mass movement deposits, which directly reach the lake shore, were observed. There is, however, no indication that such material directly reaches the coring sites in the deep northern lake basin.

Tectonics and lithologic changes also strongly affect the river catchments around Lake Towuti (Figs. 2 and 3). Steep hillslopes ($> 26^\circ$) along the Mahalona River and its tributaries north of the Matano Fault trace, in contrast to slope angles of mostly less than 5° located south of the fault (Fig. 2), suggest a strong influence of tectonics on sediment mobilisation and composition. Tectonic uplift and earthquake-triggering of slope failures in this catchment provide a constant flux of sediment to the river system, and ultimately, to the lake. Gravel deposits that accumulated in former riverbeds of the alluvial plain, observed during fieldwork, point to a sizeable contribution of remobilized sediments in the overall load that enters the lake. To the east of Lake Towuti, bedrock abrasion at the river knickpoint of the Loeha River, in combination with tectonic disturbance along a fault running parallel to the eastern lake shore (Watkinson and Hall 2016), likely explains the strong geochemical difference of the Loeha compared to the other rivers (ESM Fig. S8). As such, relatively small river catchments that are strongly influenced by tectonic disturbance can exert a strong influence on the geochemical composition of sediments deposited in the lake. Profiles of the smaller rivers to the northwest and south show no signs of recent tectonic activity, which results in a relatively low erosive capacity compared to the Mahalona and Loeha Rivers and thus a smaller influence on sediment composition at the sink.

The influence of erosional processes on lake sedimentation

The lake surface sediment geochemistry provides detailed information on the spatial variations in erosional processes and sediment composition in Lake Towuti. In areas of the lake where catchments are small and steep and valley incision is minimal, e.g. in the NE and SW, the elemental composition of the surface sediment closely resembles the laterite horizons. In these areas, slopes above the critical angle of friction are located close to the lake and mass movement processes may provide an important contribution to sedimentation. This is supported by high CIA values indicating weathered material across the western and northeastern parts of the lake compared to poorly weathered material delivered by the Mahalona and Loeha Rivers (ESM Fig. S6b). Clay mineralogy

analysis also shows a high kaolinite-to-serpentine ratio across the southern lake basin and close to the western lakeshore, where river inflow is small (Fig. 4e). In these areas, laterite material may also be mobilised and transferred into the lake by shore erosion.

Geochemistry and mineralogy of the lake sediments (Fig. 4) close to major rivers, e.g. the Mahalona, show that these rivers cut deeply through the laterite soils, transporting fresh or poorly weathered material that is derived from the bedrock and saprolite zone (ESM Fig. S8; Goudge et al. 2017). This signal is also amplified by hydrodynamic sorting in the river deltas (ESM Fig. S6; data described in detail by Hasberg et al. 2018). In addition to providing a more complete picture of the spatial extent of fluvial influence in the northern basin compared to previous studies, our results also confirm the finding by Costa et al. (2015), Vogel et al. (2015), and Goudge et al. (2017) that the Mahalona River exerts a dominant control on the present-day sediment composition of Towuti's northern basin. Our data further indicate that the mobilisation of fluvial deposits from the alluvial plains of the major rivers likely plays a role in lake sedimentation close to the river mouths.

Al/Mg as a proxy for lake level changes

The spatial patterns of chemically inert elements in the lake (e.g. Al, Mg, K, and Ti) show that today's sediment composition in the deep northern lake basin is a mixture of bedrock-derived sediments from the Mahalona River, sediments from the Loeha River, and laterite-derived input (ESM Fig. S8). In the catchment, Al, K, and Ti are enriched in the laterite horizons, whereas Mg is a characteristic element in the bedrock. Because K and Ti concentrations are relatively low ($< 1\%$ in the lake sediments; Fig. 4), the ratio of Al and Mg was chosen to represent the relative contribution of bedrock and laterite erosion in Towuti's catchment. The Al/Mg patterns (Fig. 4f) correspond to gradients in mineralogy, namely in the abundance of kaolinite and serpentine in laterite and bedrock (as expressed in the kaolinite-to-serpentine ratio). Sediments sourced from the Loeha River are characterised by higher K concentrations relative to the rivers draining ultramafic catchments (ESM Fig. S8). The chemical composition of lake sediments and the sediment cores suggests that the Loeha River has a small ($< 10\%$) but detectable influence on sediment

composition at the coring site (ESM Fig. S8). The Loeha River currently drains into the southern basin, but Costa et al. (2015) suggested that sediment from the Loeha reaches the location of core TOW9. The Al/Mg ratio at the locations of TOW9 (0.56) and Co1230 (0.87) also indicates sources other than the Mahalona River (Al/Mg of 0.15 and 0.21 in bedload and suspended load, respectively; Goudge et al. 2017), e.g. input from laterite soils (Al/Mg between 0.83 and 2.14, Fig. 3) and the Loeha River (Al/Mg = 2.62; Costa et al. 2015). Fine-grained Mahalona River sediments (Al/Mg of 0.32 and 0.37 in bedload and suspended load < 32 μm , respectively; Goudge et al. 2017) and smaller rivers entering the northern basin (Al/Mg between 0.22 and 0.28; Costa et al. 2015; ESM Fig. S8; no data available for the Timampu River) cannot account for such high values. Therefore, the Al/Mg ratio and the relation between Al–Mg–K provide information about the importance of the Mahalona relative to the Loeha River and laterite-derived sediments (ESM Fig. S8).

Although bedrock geology, tectonic processes, and erosion in the catchment regulate the general composition of sediments in the lake, this composition is modified by changes in regional hydroclimate and lake level fluctuations. Decreased lake levels lead to a lower hydrologic base level and increased hydrologic gradients, which cause deeper incision. This favours bedrock erosion relative to surficial laterite erosion, and thus a lower Al/Mg ratio of the Mahalona River during lake level low stands. Remobilisation of bedrock-derived material in the alluvial river plains during lake-level low stands favours the deposition of Mg-rich material in the deeper lake basins. Furthermore, following the interpretation of Vogel et al. (2015), a lower lake level decreases the distance between the shoreline and coring sites, causing a stronger influence of riverine suspended load and an increase in grain size at the coring locations. Because large grain sizes are enriched in Mg relative to Al (Goudge et al. 2017), this effect lowers Al/Mg during dry periods. In addition, runoff is reduced, which decreases discharge volume and long-distance sediment transport capacity of the rivers. This likely reduces the influence of the Loeha River relative to the Mahalona River, which is located much closer to the coring site. Hence, we expect a lower Al/Mg ratio in the northern lake basin during drier climate conditions. In contrast, during lake-level high stands, lower

hydrologic gradients favour a higher proportional erosion of laterite soils compared to bedrock incision, and a change from erosion to accumulation in the alluvial plains around the lake. The distance between shoreline and coring sites increases, which decreases grain size, whereas higher river discharge may increase long-distance transport capacity of the rivers, increasing the influence of the Loeha River at the coring site. These factors all increase the Al/Mg in the lake sediments during wet phases. Therefore, a high Al/Mg ratio indicates wet phases in the regional climate.

Disentangling the relative influences of tectonics and climate on lake sediment composition over time can be challenging. If fault activity in the whole lake catchment changes, sedimentation rates in the lake should change accordingly. This is not apparent in our sediment records, which span the past 60,000 years. If fault activity was enhanced along the Matano Fault, both river incision and soil erosion from steepening slopes in the river catchment should increase. If both effects were equally strong over millennial time scales, tectonic activity along the Matano Fault would not change the Al/Mg ratio in the lake significantly. In contrast, if the Loeha catchment is more strongly influenced by tectonics, K deposition at the coring sites should increase relative to Mg. This is more difficult to disentangle in the record, but an increase in kaolinite from the laterites, coinciding with an increase in K from the Loeha and a decrease in Mg from the Mahalona, would generally point towards climate (i.e. higher lake levels) rather than tectonics as the driving factor for the observed changes.

Lake Towuti's palaeoclimate record

In the past 60 kyr, Al/Mg, K, and kaolinite show similar trends in the record (Fig. 5), suggesting a dominant influence of climate processes on pelagic sedimentation in the northern basin. Changes in the past 30 kyr are seen at both coring sites, TOW9 and Co1230 (excluding event layers; Fig. 5a and b), emphasizing the homogeneity of pelagic sedimentation in the northern basin. In the past 60 kyr, the Al/Mg ratio shows lowest values in the mid-Holocene (6–4 kyr BP), in MIS2, and around 58 kyr BP (Fig. 5a). The latter two intervals correspond to glacial periods with substantial extents of northern hemisphere ice sheets. Based on data from the modern lake,

our proxy record suggests that lake level was lower and climate conditions were drier during these periods compared to today. Accordingly, high Al/Mg values in the late Holocene, at the transition from the last glacial period, and during MIS3, indicate lake level high-stands and a wet climate in Central Sulawesi. Our findings are in line with earlier studies from Lake Towuti (Russell et al. 2014; Costa et al. 2015; Vogel et al. 2015; Goudge et al. 2017), other studies from Sulawesi (Dam et al. 2001; Hope 2001; Dubois et al. 2014; Wicaksono et al. 2015, 2017), and from the Indo-Pacific Warm Pool region (De Deckker et al. 2002; Reeves et al. 2013), indicating a dry last glacial period. Vegetation around Lake Towuti, which is sensitive to climate rather than tectonics, also shows regional drying during MIS2 and wet conditions during MIS1 and MIS3 (Russell et al. 2014). These results suggest that climate was the dominant factor that shaped sedimentation in Lake Towuti over the last 60,000 years.

Interestingly, the Lake Towuti record indicates a pronounced dry period during the mid-Holocene (6–4 kyr BP) with minima in both the Al/Mg and kaolinite-to-serpentine ratios. This was described previously in a record from Lake Towuti that covered the last 45,000 years, and together with smaller variations during MIS2, was attributed to an 11-kyr, half-precessional signal (Goudge et al. 2017). Our longer, 60,000-year record suggests that during MIS3, this potential 11-kyr cyclicity is less pronounced or absent. This may be a consequence of a more dominant influence of the strong tilt of Earth's axis on northern hemisphere ice sheet extent during MIS3 (Van Meerbeeck et al. 2009; Svendsen et al. 2004; Helmens et al. 2007) and/or the influence of millennial-scale events triggered in the North Atlantic that are not resolved in our data time series (Dansgaard et al. 1993). Alternatively, other mechanisms may be responsible for the pronounced dry period during the mid-Holocene, which would require further investigation.

Conclusions

Source-to-sink analysis of the geochemistry and clay mineralogy of Lake Towuti provided insights into the modern erosional processes and sediment composition in a tropical lake catchment characterized by

ultramafic bedrock composition, lateritic soils, and active tectonics. Mass movement processes, tectonic disturbance of river profiles, and climate-induced remobilisation of fluvial deposits strongly influenced sedimentation at this site. Lower soil horizons can function as a slide plane during mass movement events, mobilising the soil package and contributing substantially to erosion in the steeper parts of this tropical catchment. In the northeastern and western lake catchment such mass movement events may supply material directly to the lake, whereas larger, tectonically disturbed rivers mainly erode and transport bedrock-derived material to the lake. Our analysis of the river profiles, along with spatially explicit analysis of surface sediment composition, added an additional, more process-based understanding of the contribution of tectonic disturbance to the sediment load delivered to the sink. In general, fault movement greatly influences the amount and dispersion of sediment delivered to the sink by disturbed, relative to less-disturbed, river systems.

Although tectonic processes and erosion in the catchment influence the general composition of the lake sediments, this composition is modified by changes in the regional hydroclimate over glacial-interglacial timescales. Based on the understanding of today's lake system, we identified the Al/Mg ratio as a proxy for lake level changes, which provide the dominant sedimentary signal for regional hydroclimate changes. Characterising and understanding the functioning of the modern lake system is crucial for the development and interpretation of sediment proxies, especially in geochemically exceptional lake systems such as Towuti. The complexity of processes described for this tropical lake catchment, in combination with the sampling and analytical approach applied, may help to inform future studies that aim to acquire information on landscape evolution in similar settings.

Acknowledgements The Towuti Drilling Project was partially supported by grants from the International Continental Scientific Drilling Program, the US National Science Foundation, the German Research Foundation, the Swiss National Science Foundation (20FI21_153054/1 and 200021_153053/1), Brown University, Genome British Columbia, and the Ministry of Research, Technology, and Higher Education (RISTEK). PT Vale Indonesia, the US Continental Drilling Coordination Office, the GeoForschungszentrum Potsdam and DOSECC Exploration Services are acknowledged for logistical assistance to the

project. We further thank Franziska Nyffenegger for support with the geotechnical analysis, Urs Eggenberger and Christine Lemp for help with the clay and bulk XRD analysis, Elias Kempf for assistance with thin section analysis, as well as Pierre Valla and Romain Delunel for fruitful discussions regarding the geomorphic aspects of the study. This research was carried out with permission from the Ministry of Research and Technology (RISTEK), the Ministry of Trade of the government of Indonesia, and the Natural Resources Conservation Center (BKSDA) and Government of Luwu Timur of Sulawesi. We also wish to thank two anonymous reviewers and the editors for their helpful comments and suggestions, which improved our manuscript.

References

- Adunoye GO (2014) Fines content and angle of internal friction of a lateritic soil: an experimental study. *Am J Eng Res* 3:16–21
- Bellier O, Sébrier M, Seward D, Beaudouin T, Villeneuve M, Putranto E (2006) Fission track and fault kinematics analyses for new insight into the Late Cenozoic tectonic regime changes in West-Central Sulawesi (Indonesia). *Tectonophysics* 413:201–220. <https://doi.org/10.1016/j.tecto.2005.10.036>
- Brand NW, Butt CRM, Elias M (1998) Nickel laterites: classification and features. *J Aust Geol Geophys* 17:81–88
- Casagrande L (1932) Research of Atterberg limits of soils. *Public Roads* 13:121–136
- Chester R, Elderfield H (1973) An infrared study of clay minerals, 2. The identification of kaolinite-group clays in deep-sea sediments. *Chem Geol* 12:281–288
- Chukanov NV (2014) *Infrared spectra of mineral species*. Springer, Dordrecht
- Colin F, Nahon D, Trescases JJ, Melfi AJ (1990) Lateritic weathering of pyroxenites at Niquelandia, Goiás, Brazil: the supergene behavior of nickel. *Econ Geol* 85:1010–1023
- Costa KM, Russell JM, Vogel H, Bijaksana S (2015) Hydrological connectivity and mixing of Lake Towuti, Indonesia in response to paleoclimatic changes over the last 60,000 years. *Palaeogeogr Palaeoclimatol Palaeoecol* 417:467–475. <https://doi.org/10.1016/j.palaeo.2014.10.009>
- Crowe SA, Jones C, Katsev S, Magen C, O'Neill AH, Sturm A, Canfield DE, Haffner GD, Mucci A, Sundby B, Fowle DA (2008) Photoferrotrophs thrive in an Archean Ocean analogue. *Proc Natl Acad Sci USA* 105:15938–15943. <https://doi.org/10.1073/pnas.0805313105>
- Dam RAC, Fluin J, Suparan P, van der Kaars S (2001) Palaeoenvironmental developments in the Lake Tondano area (N. Sulawesi, Indonesia) since 33,000 yr BP. *Palaeogeogr Palaeoclimatol Palaeoecol* 171:147–183
- Dansgaard W, Johnsen SJ, Clausen HB, Dahl-Jensen D, Gundstrup NS, Hammer CU, Hvidberg CS, Steffensen JP, Sveinbjörnsdóttir AE, Jouzel J, Bond G (1993) Evidence for general instability of past climate from a 250-kyr ice-core record. *Nature* 364:218–220
- De Deckker P, Tapper NJ, van der Kaars S (2002) The status of the Indo-Pacific Warm Pool and adjacent land at the last glacial maximum. *Glob Planet Chang* 35:25–35
- DIN 18137-1. German Industrial Norm (2010) *Baugrund, Untersuchung von Bodenproben. Bestimmung der Scherfestigkeit, Teil 1: Begriffe und grundsätzliche Versuchsbedingungen* [Soil, investigation and testing—Determination of shear strength—Part 1: Concepts and general testing conditions]
- DIN 18137-3. German Industrial Norm (2002) *Baugrund, Untersuchung von Bodenproben. Bestimmung der Scherfestigkeit, Teil 3: Direkter Scherversuch* [Soil, investigation and testing - Determination of shear strength - Part 3: Direct shearing test]
- Dubois N, Oppo DW, Galy VV, Mohtadi M, van der Kaars S, Tierney JE, Rosenthal Y, Eglinton TI, Lückge A, Linsley BK (2014) Indonesian vegetation response to changes in rainfall seasonality over the past 25,000 years. *Nat Geosci* 7:513–517. <https://doi.org/10.1038/ngeo2182>
- Farmer VC (1974) *The infrared spectra of minerals*. Adlard and Son, Dorking
- Golightly JP, Arancibia ON (1979) The chemical composition and infrared spectrum of nickel- and iron-substituted serpentine from a nickeliferous laterite profile, Soroako, Indonesia. *Can Miner* 17:719–728
- Goudge TA, Russell JM, Mustard JF, Head JW, Bijaksana S (2017) A 40,000 yr record of clay mineralogy at Lake Towuti, Indonesia: paleoclimate reconstruction from reflectance spectroscopy and perspectives on paleolakes on Mars. *Bull Geol Soc Am* 129:806–819. <https://doi.org/10.1130/B31569.1>
- Haffner GD, Hehanussa PE, Hartoto D (2001) The biology and physical processes of large lakes of Indonesia: Lakes Matano and Towuti. In: Munawar M, Hecky RE (eds) *The Great Lakes of the World (GLOW)*. Michigan State University Press, pp 183–192
- Hasberg AKM, Melles M, Wennrich V, Just J, Held P, Morlock MA, Vogel H, Russell JM, Bijaksana S, Opitz S (2018) Modern sedimentation processes in Lake Towuti, Indonesia, revealed by the composition of surface sediments. *Sedimentology*. <https://doi.org/10.1111/sed.12503>
- Helmens KF, Bos JAA, Engels S, Van Meerbeeck CJ, Bohncke SJP, Renssen H, Heiri O, Brooks SJ, Seppä H, Birks HJB, Wohlfarth B (2007) Present-day temperatures in northern Scandinavia during the last glaciation. *Geology* 35:987–990. <https://doi.org/10.1130/G23995S1>
- Hope G (2001) Environmental change in the Late Pleistocene and later Holocene at Wanda site, Soroako, South Sulawesi, Indonesia. *Palaeogeogr Palaeoclimatol Palaeoecol* 171:129–145
- Jones ES, Hayes GP, Bernardino M, Dannemann FK, Furlong KP, Benz HM, Villaseñor A (2014) Seismicity of the Earth 1900–2012, Java and vicinity. U.S. Geological Survey Open-File Report 2010–1083-N, 1 sheet, scale 1:5,000,000. <https://doi.org/10.3133/ofr20101083n>
- Kadarusman A, Miyashita S, Maruyama S, Parkinson CD, Ishikawa A (2004) Petrology, geochemistry and paleogeographic reconstruction of the East Sulawesi Ophiolite, Indonesia. *Tectonophysics* 392:55–83. <https://doi.org/10.1016/j.tecto.2004.04.008>

- Konecky B, Russell JM, Bijaksana S (2016) Glacial aridity in central Indonesia coeval with intensified monsoon circulation. *Earth Planet Sci Lett* 437:15–24. <https://doi.org/10.1016/j.epsl.2015.12.037>
- Madejová J (2003) FTIR techniques in clay mineral studies. *Vib Spectrosc* 31:1–10
- Marsh E, Anderson E, Gray F (2013) Nickel–cobalt laterites—a deposit Model. In: Mineral deposit models of resource assessment. U.S. Geological Survey, Reston, USA
- Nesbitt HW, Young GM (1982) Early Proterozoic climates and plate motions inferred from major element chemistry of lutites. *Nature* 299:715–717
- Ogunsanwo O (1988) Basic geotechnical properties, chemistry and mineralogy of some laterite soils from S.W. Nigeria. *Bull Int Assoc Eng Geol* 37:131–135
- Omotoso OA, Ojo OJ, Adetolaju ET (2012) Engineering properties of lateritic soils around Dall Quarry in Sango Area, Ilorin, Nigeria. *Earth Sci Res* 1:71–81. <https://doi.org/10.5539/esr.v1n2p71>
- R Development Core Team (2008) R: a language and environment for statistical computing. R Foundation for Statistical Computing. www.r-project.org. Accessed 13 Feb 2017
- Reeves JM, Bostock HC, Ayliffe LK, Barrows TT, De Deckker P, Devriendt LS, Dunbar GB, Drysdale RN, Fitzsimmons KE, Gagan MK, Griffiths ML, Haberle SG, Jansen JD, Krause C, Lewis S, McGregor HV, Mooney SD, Moss P, Nanson GC, Purcell A, van der Kaars S (2013) Palaeoenvironmental change in tropical Australasia over the last 30,000 years—a synthesis by the OZ-INTIMATE group. *Quat Sci Rev* 74:97–114. <https://doi.org/10.1016/j.quascirev.2012.11.027>
- Robinson GW (1922) A new method for the mechanical analysis of soils and other dispersions. *J Agric Sci* 12:306–321
- Russell JM, Vogel H, Konecky B, Bijaksana S, Huang Y, Melles M, Wattrus N, Costa KM, King JW (2014) Glacial forcing of central Indonesian hydroclimate since 60,000 y BP. *PNAS* 111:5100–5105. <https://doi.org/10.1073/pnas.1402373111>
- Russell JM, Bijaksana S, Vogel H, Melles M, Kallmeyer J, Ariztegui D, Crowe S, Fajar S, Hafidz A, Haffner D, Hasberg A, Ivory S, Kelly C, King J, Kirana K, Morlock M, Noren A, O’Grady R, Ordóñez L, Stevenson J, von Rintelen T, Vuillemin A, Watkinson I, Wattrus N, Wicaksono S, Wonik T, Bauer K, Deino A, Friese A, Henny C, Imran Marwoto R, Ngkoimani LO, Nomosatryo S, Safiuddin LO, Simister R, Tamuntuan G (2016) The Towuti Drilling Project: paleoenvironments, biological evolution, and geomicrobiology of a tropical Pacific lake. *Sci Drill* 21:29–40. <https://doi.org/10.5194/sd-21-29-2016>
- Sagapoa CV, Imai A, Watanabe K (2011) Laterization process of ultramafic rocks in Siruka, Solomon Islands. *J Nov Carb Resour Sci* 3:32–39
- SN 670 010. Swiss Norm. Geotechnische Erkundung und Untersuchung—Geotechnische Kenngrößen [Geotechnical exploration and analysis—Geotechnical parameters]. Edition 2011-08
- SN 670 902-1 (EN 933-1). Swiss Norm. Prüfverfahren für geometrische Eigenschaften von Gesteinskörnungen. Teil 1: Bestimmung der Korngrößenverteilung—Siebverfahren [Testing geometric properties of grains, Part 1: Grain-size distribution—Sieving]. Edition 2013-03
- Svendsen JI, Alexanderson H, Astakhov VI, Demidov I, Dowdeswell JA, Funder S, Gataullin V, Henriksen M, Hjort C, Houmark-Nielsen M, Hubberten HW, Ingólfsson Ó, Jakobsson M, Kjær KH, Larsen E, Lokrantz H, Lunkka JP, Lyså A, Mangerud J, Matiouchkov A, Niessen F, Nikolskaya O, Polyak L, Saarnisto M, Siegert C, Siegert MJ, Spielhagen RF, Stein R (2004) Late quaternary ice sheet history of northern Eurasia. *Quat Sci Rev* 23:1229–1271. <https://doi.org/10.1016/j.quascirev.2003.12.008>
- Thomas MF (1996) *Geomorphology in the tropics*. Wiley, Chichester
- U.S. Geological Survey (2017) Mineral commodity summaries 2017. U.S. Geological Survey, Reston. <https://doi.org/10.3133/70180197>
- Van Meerbeeck CJ, Renssen H, Roche DM (2009) How did marine isotope stage 3 and last glacial maximum climates differ?—Perspectives from equilibrium simulations. *Clim Past* 5:33–51
- Vogel H, Russell JM, Cahyarini SY, Bijaksana S, Wattrus N, Rethemeyer J, Melles M (2015) Depositional modes and lake-level variability at Lake Towuti, Indonesia, during the past ~ 29 kyr BP. *J Paleolimnol* 54:359–377. <https://doi.org/10.1007/s10933-015-9857-z>
- Von Rintelen T, Von Rintelen K, Glaubrecht M, Schubart CD, Herder F (2012) Aquatic biodiversity hotspots in Wallacea: the species flocks in the ancient lakes of Sulawesi, Indonesia. In: Gower DJ, Johnson K, Richardson J, Rosen B, Rüber L, Williams S (eds) *Biotic evolution and environmental change in Southeast Asia*. Cambridge University Press, Cambridge, pp 291–315
- Watkinson IM, Hall R (2016) Fault systems of the eastern Indonesian triple junction: evaluation of Quaternary activity and implications for seismic hazards. In: Cummins PR, Meilano I (eds) *Geohazards in Indonesia: Earth science for disaster risk reduction*. Geological Society, London, pp 71–120
- Weber AK, Russell JM, Goudge TA, Salvatore MR, Mustard JF, Bijaksana S (2015) Characterizing clay mineralogy in Lake Towuti, Indonesia, with reflectance spectroscopy. *J Paleolimnol* 54:253–261. <https://doi.org/10.1007/s10933-015-9844-4>
- Whipple KX, Kirby E, Brocklehurst SH (1999) Geomorphic limits to climate-induced increases in topographic relief. *Nature* 401:39–43. <https://doi.org/10.1038/43375>
- Wicaksono SA, Russell JM, Bijaksana S (2015) Compound-specific carbon isotope records of vegetation and hydrologic change in central Sulawesi, Indonesia, since 53,000 yr BP. *Palaeogeogr Palaeoclimatol Palaeoecol* 430:47–56. <https://doi.org/10.1016/j.palaeo.2015.04.016>
- Wicaksono SA, Russell JM, Holbourn A, Kuhnt W (2017) Hydrological and vegetation shifts in the Wallacean region of central Indonesia since the Last Glacial Maximum. *Quat Sci Rev* 157:152–163. <https://doi.org/10.1016/j.quascirev.2016.12.006>
- Widdowson M (2007) Laterite and ferricrete. In: Nash DJ, McLaren SJ (eds) *Geochemical sediments and landscapes*. Blackwell Publishing, Malden, pp 46–94
- SN 670 816a. Swiss Norm. Mineralische Baustoffe, Schlamm-analyse nach der Aräometermethode [Minerogenic material—Sieving analysis by aerometric method]
- SN 670 345b. Swiss Norm. Böden—Konsistenzgrenzen [Soils—Plasticity Index]